In the CO_2 emission remediation by means of alternative geopolymers as substitutes for cements

C. Carreño-Gallardo[a], A. Tejeda-Ochoa[a], O.I. Perez-Ordonez[a], J.E. Ledezma-Sillas[a],
D. Lardizabal-Gutierrez[a], C. Prieto-Gomez[b], J.A. Valenzuela-Grado[b], F.C. Robles Hernandez[c],
J.M. Herrera-Ramirez[a],[*]

[a] Centro de Investigación en Materiales Avanzados (CIMAV), Laboratorio Nacional de Nanotecnología, Miguel de Cervantes 120, Chihuahua, Chih., 31136, Mexico
[b] Grupo Cementos de Chihuahua, Vicente Suarez y 6a. S/N, Chihuahua, Chih., 31110, Mexico
[c] Department of Mechanical Engineering Technology, University of Houston, Houston, TX 77204-4020, USA

ARTICLE INFO

ABSTRACT

Here we present a geopolymer as a sustainable alternative for cements. The geopolymer binder is presented in a dry form (dry mixing method). The geopolymer has demonstrated to be ideal candidate to mitigate the typical carbon footprint emissions of cements, such as Portland. The potential global benefits include a reduction of up to 1480 million tons of CO_2 per year when compare with Portland cement. In this design, it is proposed an alkali-activated cementitious material that is made out of a mix of silica-rich sand and sodium carbonate. Such sand has 80–85 wt% SiO_2 and 15–20 wt% mixed rock grain. This composition is processed at temperatures around 850 °C that is 650 °C less than that for Portland cements. One of the benefits is that the use of limestone is eliminated resulting in such reductions in CO_2 emissions. The emission analysis is carried during a calcination process used to analyze the decarbonation or CO_2 emission step. This work presents a complementary characterization of the products including an infrared spectroscopy analysis and thermogravimetry.

1. Introduction

Ordinary Portland Cement (OPC) is the most common hydraulic binder used in civil infrastructure. The OPC is known for more than 150 years [1]. The OPC is obtained by calcining a mixture of limestone ($CaCO_3$) and clay at around 1500 °C followed by a grinding process. The product is known as clinker. Once the clinker is ground, it is mixed with 5–8 wt% of gypsum to form the cement. Gypsum, among other effects controls the curing speed of the cement [1–5]. Geopolymers are an innovative alternative to replace the Portland cement, which are environmentally friendly, have a high level of workability, and are more resistant to chemical and high-temperature environments [6–8].

Fig. 1 presents diagrams comparing the processing steps for both the OPC and the geopolymer. The cement manufacturing process requires several processing steps and each step has an associate energy that is sketched in Fig. 1a. In general terms, the energy requirements to produce a metric ton of clinker is approximately 6 GJ. The raw materials requirements to produce a ton of cement is approximately 1.7 tons of limestone and clay [9]. Every ton of cement generates between 0.66 and 0.82 tons of CO_2, which depends on the characteristics of the raw

materials and fuels [10,11]. In accordance with the International Energy Agency (IEA), the global CO_2 emissions will be around 28,000 millions of tons in the year 2050 [12]. The OPC contributes with 5–10 wt% of the global anthropogenic emissions, particularly CO_2 [5,10,12–16].

The main sources of the CO_2 emissions in the OPC are attributed to the calcination of limestone. The CO_2 generated is a byproduct that accounts not only the emissions of the OPC, but also those of the burned fuels [13,14]. Eq. (1) describes the typical thermal decomposition reaction during calcination of limestone:

$$CaCO_3 \xrightarrow{\Delta} CaO + CO_2 \tag{1}$$

Davidovits [17] is considered to be the first in producing a geopolymer by using aluminosilicate powder with an alkaline solution. In recent years, geopolymers have attracted significant attention because they offer early compressive strength (relatively fast curing), low permeability, good chemical resistance and excellent fire resistance [18]. The compressive strength of the geopolymer allows to subject it to compressive forces as early as 7 days after curing initiates. Geopolymers are an alternative cementitious binder, comprising of an alkali activated

---

[*] Corresponding author.
 E-mail address: martin.herrera@cimav.edu.mx (J.M. Herrera-Ramirez).
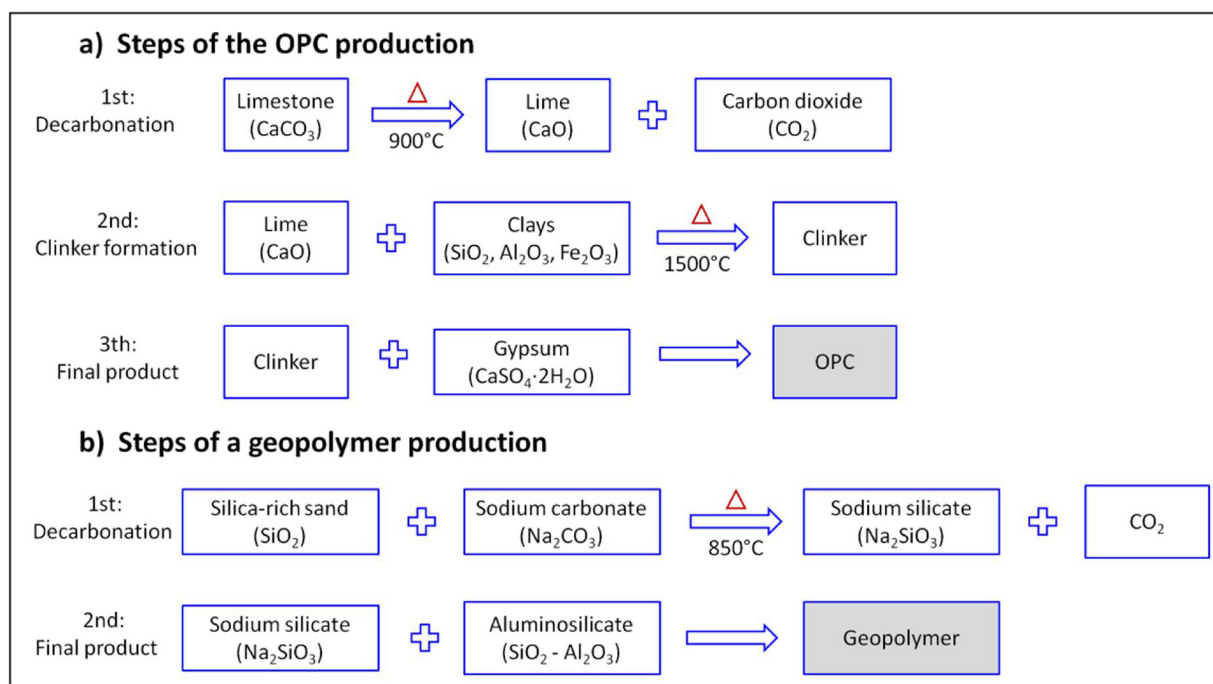
Fig. 1. Flow sketching the production of (a) ordinary Portland cement and (b) the geopolymer.

with an aluminosilicate that are considered the substitute for OPC [19]. A geopolymer cement hardens at room temperatures, having a compressive strengths of 20 MPa after only 4 h and up to 70–100 MPa after 28 days [19].

The geopolymers are produced with aluminosilicates (Al_2O_3-SiO_2) sources, which may contain calcite ($CaCO_3$) and ferric oxide (Fe_2O_3) in smaller amounts [20]. Geopolymers require an alkaline activator that induces the pozzolanic activation and accelerates the geopolymerization process. Sodium silicate (Na_2SiO_3) is well known for its advantage as an activator of geopolymers [13,20–22]. It is necessary to produce Na_2SiO_3 to obtain the geopolymers, since the aluminosilicates sources are usually obtained as a waste or an industrial byproduct. Fig. 1b shows the geopolymers production process, where the Na_2SiO_3 is obtained from silica-rich sands and Na_2CO_3. This process is the main contributor to the anthropogenic emissions generated. Eq. (2) summarizes the process.

$$Na_2CO_3 + SiO_2 \xrightarrow{\Delta} Na_2SiO_3 + CO_2 \qquad (2)$$

It is worth mentioning that once the Na_2SiO_3 is produced the geopolymer if formed by mixing it with the aluminosilicate. In other words, the final product does not require heat or calcination, it is purely mechanical integration and therefore no emissions are associated by this stage. As a result, this minimizes the energy requirements and the unwanted CO_2 emissions. Hence, the maximum temperature requirement to produce the geopolymer is 850 °C. In contrast the production of the OPC requires a calcination process at around 1500 °C to form the clinker.

Here it is demonstrated analytically and experimentally, the environmental benefits of the geopolymer when compared to a commercial OPC. The main two aspects of the present work are the limited emissions in the decarbonation process in the geopolymer as well as the significantly lower temperature requirements (Fig. 1). In this research are presented the evidences that make a clear distinction in the decarbonation step for both products. The analytical results are here supported with experimental work by means of thermogravimetry and infrared spectroscopy.

2. Materials and methods

The experimental procedure is divided in the following steps: synthesis of materials, identification of the anthropogenic emissions by infrared spectroscopy, quantification of the emissions by thermogravimetry (TGA) and gravimetry method, quantification of the energy involved in the Na_2CO_3 and $CaCO_3$ decomposition by DSC, and mechanical properties of finished products.

2.1. Synthesis of materials

The raw materials to produce Na_2SiO_3 are silica-rich sand and industrial-grade sodium carbonate. Scanning electron microscopy (SEM) is used to observe the morphology of raw materials and cements; a Hitachi SU3500 microscope operated at 15 kV and 150 µA is used. The elemental makeup of the sand used in this work is composed of Si, O, Al, K, Fe, Na, and Ca, and an estimated concentration is determined by energy dispersive X-ray spectroscopy (EDS) coupled to the Hitachi SU3500 microscope. Taking into account that the EDS analysis is a semiquantitative technique, complementary analysis are made by X-ray fluorescence (XRF) in order to determine the oxide chemical composition of the materials; a Philips Cubix XRF Dy699 apparatus provided with a 200 W Sc tube target, operated at 50 kV and 4 mA, is used. The X-ray diffraction (XRD) result confirms that the predominant phase is quartz (SiO_2). For the XRD analysis, a Panalytical X'Pert PRO diffractometer with X'Celerator detector is used, under a Cu Kα radiation ($\lambda = 0.15418$ nm), at 40 kV and 30 mA in the 2θ range of 10-80°; the step and acquisition time are 0.015° and 120 s, respectively.

The particle size distribution of the materials is determined using a particle size analyzer CILAS 1180. The samples are dissolved in isopropyl alcohol to have alcohol/aqueous suspensions (20:80). This equipment uses the laser diffraction and a CCD camera, which allows, in one single range, the measurement of particles between 0.04 and 2500 µm. The fine particles are measured by the diffraction pattern using Fraunhofer or Mie theory. The coarse particles are measured using a real-time fast Fourier transform of the image obtained with a CCD camera equipped with a digital signal-processing unit.
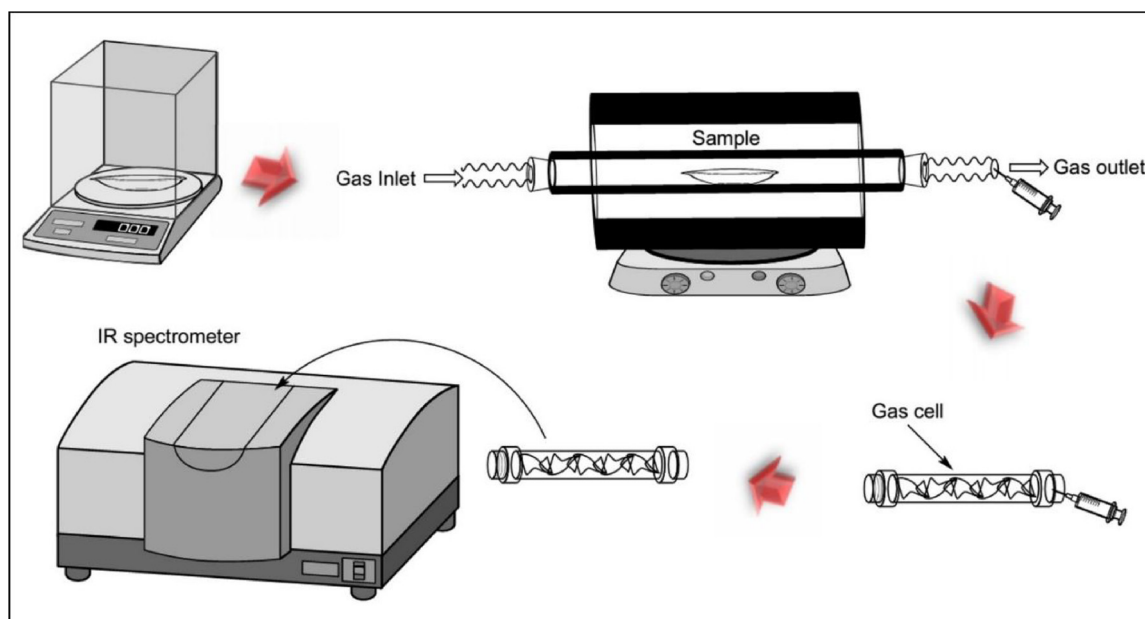
Fig. 2. Steps for the capture and analysis of gases emitted during the decarbonation reaction for producing Na_2SiO_3 and clinker.

2.2. Infrared spectroscopy

Firstly, raw materials were dried at 500 °C in a Barnstean Thermolyne 6000 furnace for 2 h. Then the mixtures were placed inside a quartz tube and treated in a Thermolyne 21100 furnace. The quartz tube is sealed and the gases are manipulated via gas flow inlet and outlet. Argon is blown during the process as a carrier to collect the emissions.

In the first step the products are heated to 120 °C for 5 min blowing argon at a rate of 50 mL/min. This step is done to eliminate any potential leftover humidity. After that, the temperature is raised to 950 °C in the absence of gas. At the end of the process the gases are collected in the outlet with a syringe, and analyzed in a Thermo/Nicolet Magna-IR 750 spectrometer. The infrared spectra are obtained by passing the gases generated in the pyrolysis through a 10-cm-long gas chamber provided with a zinc selenide window. The gases generated are dragged by a 40 cm^3/min N_2 flow (99.999% purity, Praxair); 100 measurements are made per temperature interval, with a resolution of 4 cm. Fig. 2 sketches the respective procedure.

2.3. Thermogravimetry (TGA)

The TGA test was carried in a TA Instrument Q600 thermobalance. Here is measured quantitatively the emissions during calcination of Na_2CO_3 and $CaCO_3$. The analyzed samples weigh approximately 10 mg. The process is carried in an argon atmosphere (50 mL/min) at a rate of 10 °C/min until 950 °C. The mass loss is determined directly from the TGA thermograms.

2.4. Gravimetry

The gravimetry test is carried in compliance with the ASTM C114-15 standard [23] for both mixtures. In both cases, mixes of 1 g are introduced in a crucible previously dried to constant weight. Next, the mixtures are heated to 500 °C for 2 h in a Barnstean Thermolyne 6000 furnace. This process helps eliminating the presence of humidity and OH species. The treated product is then cooled to room temperature in a desiccator. The products are weighted once they are at room temperature. The crucibles are then heated to 950 °C for 2 h. Those conditions were established to ensure complete decarbonation. The crucibles are again allowed to reach standard conditions in a desiccator and

then weighted. The difference in weight is attributed to the emissions (CO_2).

2.5. Energy analysis

The differential scanning calorimetry (DSC) analysis is used to determine the energy needed for the decarbonation during the Na_2SiO_3 and clinker production. This study is performed by means of DSC to determine the energies needed to complete the chemical reactions. The chemical reactions are calculated directly from the integral between the baseline and the first derivative of the cooling or heating curve(s) and they can be endo or exothermic. In the case of the decarbonation process the reactions are expected to be exothermic.

2.6. Mechanical properties

In order to evaluate the feasibility of using geopolymers as substitutes for cements, pastes and mortars of both geopolymer and ordinary cement are synthesized through different formulations, in accordance with the ASTM C305-14 standard. The mixtures are poured into 50-mm cubic molds. The pastes and mortars are tested by compression tests after 7, 14 and 28 days of curing, according to the ASTM C109/C109M-16a standard. The tests are carried out in an Instron universal testing machine with a load cell of 50 ton; a head speed of 12 mm/min is used.

3. Results and discussion

According to the results of the chemical analysis performed by EDS, the composition (in wt%) of the sand is Si: 69.3, O: 20.7, Al: 4.3, K: 2.5, Fe: 2.3 Na: 0.8 and Ca: 0.3. The results of XRD (Fig. 3) allowed to determine the phases Sanidine ($K(AlSi_3)O_8$) and Albite $Na(AlSi_3O_8)$. The percentage of SiO_2 contained in the sand was considered in the calculation for producing Na_2SiO_3 (Eq. 2), and the sand is composed of 82.28 wt% of silica quartz. In addition, XRF allowed to determine the oxide chemical composition of the sand, Na_2SiO_3 and clinker, which are summarized in Table 1. Fig. 4a presents a micrograph of Na_2SiO_3, which consists of small fibrous particles agglomerated all together. Fig. 4b shows that clinker has an irregular morphology, with variable particle size. The particle size analyzer allows seeing that the average particle size of Na_2SiO_3 is 197.14 ± 18; even though the sodium
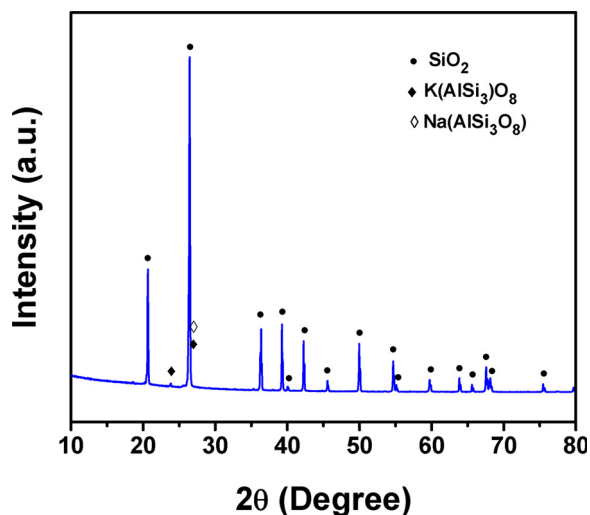
Fig. 3. XRD pattern of the sand.

Table 1
Oxides composition (wt%) of the materials.

Material	SiO$_2$	Al$_2$O$_3$	Na$_2$O	Fe$_2$O$_3$	CaO	MgO	K$_2$O	SO$_3$
Sand	82.28	9.10	3.38	1.51	0.79	0.07	2.68	0.19
Na$_2$SiO$_3$	60.44	7.62	28.58	0.99	0.38	0.05	1.86	0.08
Clinker	21.00	4.90	0.13	3.48	66.82	2.77	0.56	0.34

silicate consists of small particles (Fig. 4a), they are agglomerated causing the equipment to detect a much larger particle size. The average particle size of clinker is 15.54 ± 6.

3.1. Infrared spectroscopy

Fig. 5 shows the IR spectra for the gas emitted by the synthesis of Na$_2$SiO$_3$ and clinker. The absorption bands confirmed the presence of CO$_2$ with compliance to the characteristic bending and stretching bands [24]. The band observed at 2640 cm^{-1} belongs to the C=O stretching and that at 669 cm^{-1} belongs to the O=C=O bending. Both vibrational modes are also sketched for easier identification. The combinatorial modes $v_1 + v_3$ and $2v_2 + v_3$ are identified at 3717 and 3607 cm^{-1}, respectively. The IR analysis is qualitative and should not be interpreted based on the proportionality of the spectra intensities. Instead, the difference between the spectra in Fig. 5 only demonstrates the CO$_2$ relative concentrations in the samples.

3.2. Thermogravimetry (TGA)

The results in Fig. 6 correspond to the TGA analysis for the raw

materials calcination to produce the Na$_2$SiO$_3$ and we compare the results to those of the clinker production. Two changes of mass loss occurred before calcination. The first change in the slope (also understood as a mass reduction) occurs when the sample is heated between 100 and 150 °C; that is attributed to water. The second mass one occurs from 200 to 450 °C, which corresponds to a degradation of the OH species linked to silicon. The mass loss after 550 °C is the decarbonation reaction or CO$_2$ generation with a respective mass loss of 34.21 wt% in the clinker and only 23.67 wt% in the Na$_2$SiO$_3$.

Comparing the differences between the Na$_2$SiO$_3$ (23.67 wt%) and clinker (34.21 wt%), it may be concluded that the CO$_2$ emissions in Na$_2$SiO$_3$ are approximately 31 wt% less than those in the clinker. Those results were further confirmed by the mass change in both cases. To make a brief comparison, a kilogram of clinker produces 0.342 kg of CO$_2$, while that a kilogram of Na$_2$SiO$_3$ produces only 0.237 kg of CO$_2$.

3.3. Gravimetry

The results of direct gravimetric show that the Na$_2$SiO$_3$ production generates 23.56 wt% CO$_2$, while the clinker one generates 34.27 wt% CO$_2$. Comparing these two values it is clear that the CO$_2$ produced by Na$_2$SiO$_3$ is 31% less than that produced by the clinker. These stoichiometric mass balance and the TGA results are in agreement. The tests are done using thermogravimetry and gravimetry with samples of approximately 10 mg and 1 g, respectively. This work is performed to demonstrate that the results are somehow scalable from the micro to the meso levels and it is expected that is does extrapolate to the macro level.

3.4. Energy analysis

The heat energy balance was carried out using differential scanning calorimetry (DSC) where we also identified the decomposition reaction occurring during the heating process. The transformation reactions (endothermic peaks) during decarbonation for each sample are observed in Fig. 7. In the case of the clinker, the products of decarbonatation of CaCO$_3$ are CaO and CO$_2$ (see Eq. (1)). The Na$_2$SiO$_3$ is the product of a combination of Na$_2$CO$_3$ and SiO$_2$ with a balanced of CO$_2$ (Eq. (2)). Fig. 7 shows that the latent heat of transformation for Na$_2$O$_3$Si where it can be seen a significant reduction when compared to the clinker. This is translated into less demanding energy requirements for the decarbonation process. The energy requirements to produce the Na$_2$SiO$_3$ are 0.306 kJ/g and for the clinker is 1.059 kJ/g. These values can be expressed as 0.085 and 0.294 kW h/kg, respectively (Table 2). This suggests less demanding energy needs as well as CO$_2$ emissions.

The above results are further confirmed with the following analytical procedure, using a sample size of 1 kg (Na$_2$SiO$_3$ or clinker). According to the Asociacion de Tecnicos y Profesionistas en Aplicacion Energetica (ATPAE) [25], for every MWh generated, 0.6539 ton of CO$_2$ are emitted to the environment. Therefore, the kWh supplied for the Na$_2$SiO$_3$ production generate 0.056 kg of CO$_2$, and for the same amount
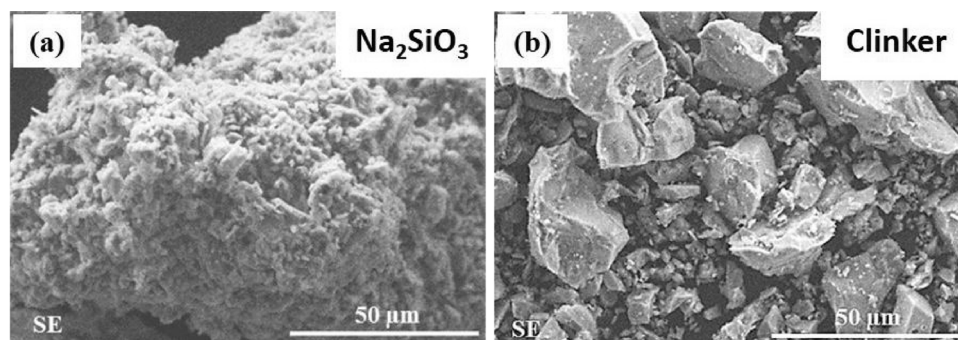

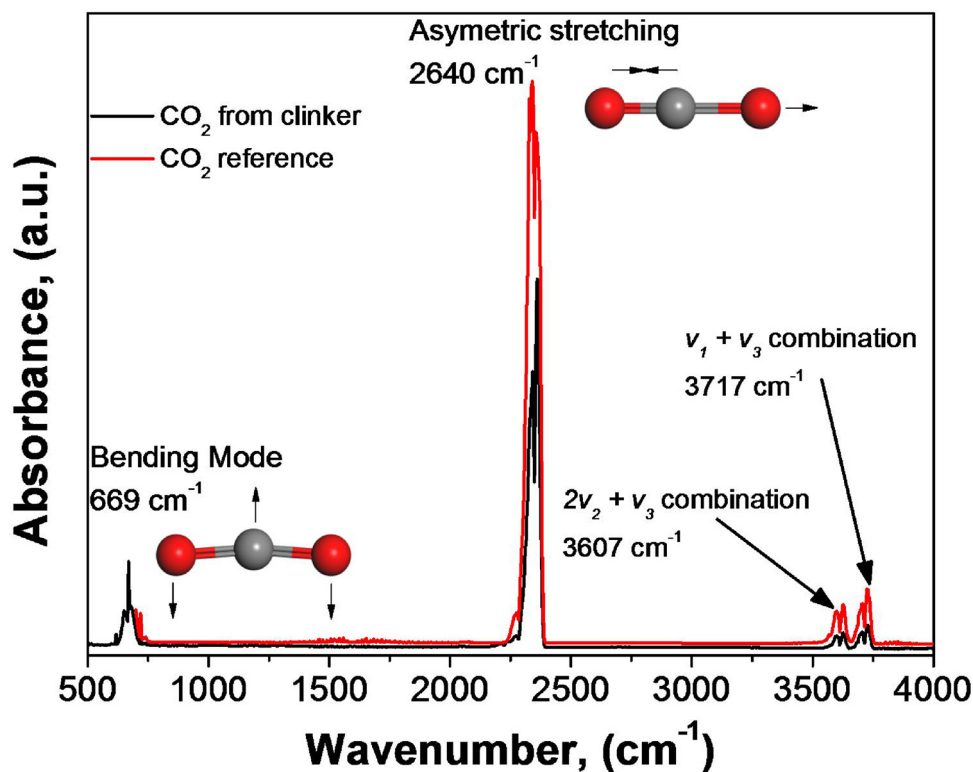**Fig. 4.** SE-SEM micrographs of (a) Na$_2$SiO$_3$ and (b) clinker.

Fig. 5. Spectrum of the gas emitted during the decarbonation of the clinker production, compared with the CO_2 standard spectrum.
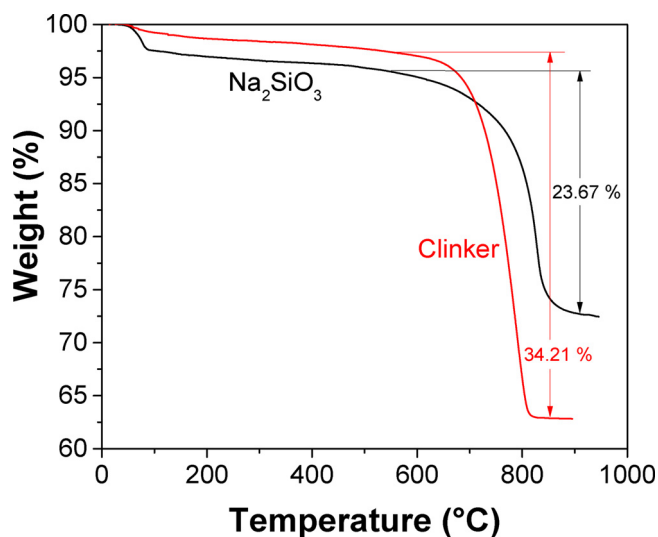

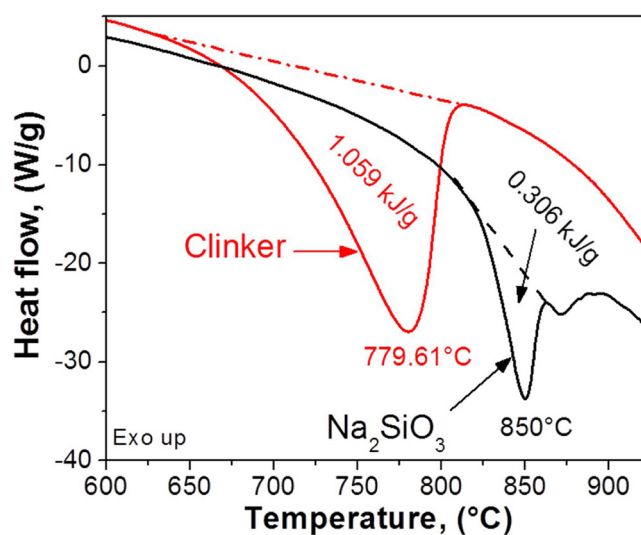**Fig. 6.** Thermogravimetry results of the Na_2SiO_3 and clinker production.

Fig. 7. Energy required to produce Na_2SiO_3 and clinker.

of clinker the CO_2 emitted is 0.192 kg. If these values are added to the CO_2 mass generated from the decarbonation reaction, Na_2SiO_3 and the clinker generate 0.237 kg and 0.342 kg of CO_2, respectively. Adding this up to the decarbonation, it is obtained 0.293 kg in the case of Na_2SiO_3 and 0.534 kg for the clinker per kg of sample. Table 2 shows all these calculations. Yet, in summary one can say that Na_2SiO_3 generates 45% less CO_2 than the clinker.

Our results are in agreement with those in the literature [26,27]. Nelson [26] states that the required energy to produce clinker at the step of decarbonation is 1974 kJ/kg (0.548 kW h) with 0.359 kg of CO_2 emitted. On the other hand, Hasanbeigi et al. [27] report 0.540 kg of CO_2 emitted. Additionally, it is known that the production of 1 kg of OPC generates 1 kg of CO_2 [27].

It is worth emphasizing again that our calculations are only for the

Table 2
Calculation of the total CO_2 emission during the Na_2SiO_3 and clinker production.

Unit	Na_2SiO_3	Clinker
kJ/g	0.306	1.059
kWh/kg	0.085	0.294
kg CO_2 (Energy)	0.056	0.192
kg CO_2 (Decarbonation)	0.237	0.342
Total kg CO_2 emitted	**0.293**	**0.534**

decarbonation step of both products. It is expected that, comparatively, the energy and emissions due to clincker synthesis are superior; unfortunately, to generate this data one need specialized systems that
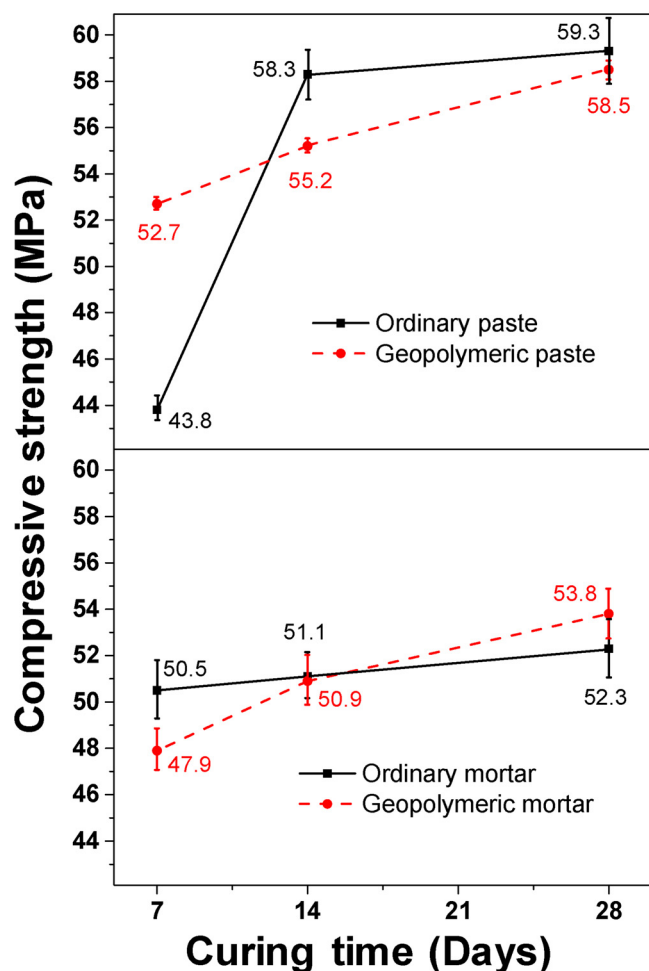
Fig. 8. Compressive strength of pastes and mortars as a function of curing time.

require working temperatures of 1500 °C or higher. However, Nelson [26] claims that to heat the clinker from 900 to 1450 °C in a rotary kiln we need 0.544 kJ/g (0.151 kW h/kg), which generates 0.099 kg CO_2. Therefore, if 0.099 kg CO_2 are added to 0.534 kg CO_2 reported in Table 2, a total of 0.633 kg CO_2 are calculated to be emitted for the whole clinker production. This allows to conclude that the geopolymer obtained in this work generates 54% less CO_2 than the Portland cement clinker.

Because the OPC has been being manufactured for years, a lot of information about it is available in the literature. For instance, it is reported that the production of 1 ton of ordinary Portland cement generates 1 ton of CO_2 [27], which derives from i) Decarbonation: 55% (540 kg), ii) Combustion: 35% (340 kg) and iii) Energy (others): 10% (120 kg). This is, about 55% of the CO_2 emissions comes from decarbonation reactions occurring in the furnace, while about 35% comes from the energy consumption necessary to raise the temperature of the material to more than 1450 °C; the rest comes from the energy and transportation related to the production and dispatch process.

It is worth noting that this investigation is focused in the decarbonation step of both materials, leaving aside the CO_2 emissions from the 'Combustion' and 'Energy'. Taking this into account, the 0.534 kg of CO_2 generated per kg of clinker produced (Table 2), are exclusively coming from the decarbonation step, which are in very good agreement with the amount described above. In the case of the geopolymeric materials, there is no data to be able to compare our results; this is, with our work we are generating data experimentally. However, the good agreement between our results and those empirical for the clinker allows us to say that 0.293 kg of CO_2 are generated per kg of Na_2SiO_3 produced (Table 2).

3.5. Mechanical properties

Fig. 8 shows the compression tests results of pastes and mortars, both ordinary and geopolymeric materials, after 7, 14 and 28 days of curing. The results presented correspond to samples with the highest compressive strength of all the formulations synthesized. As can be seen, after 28 days of curing the geopolymeric materials have a
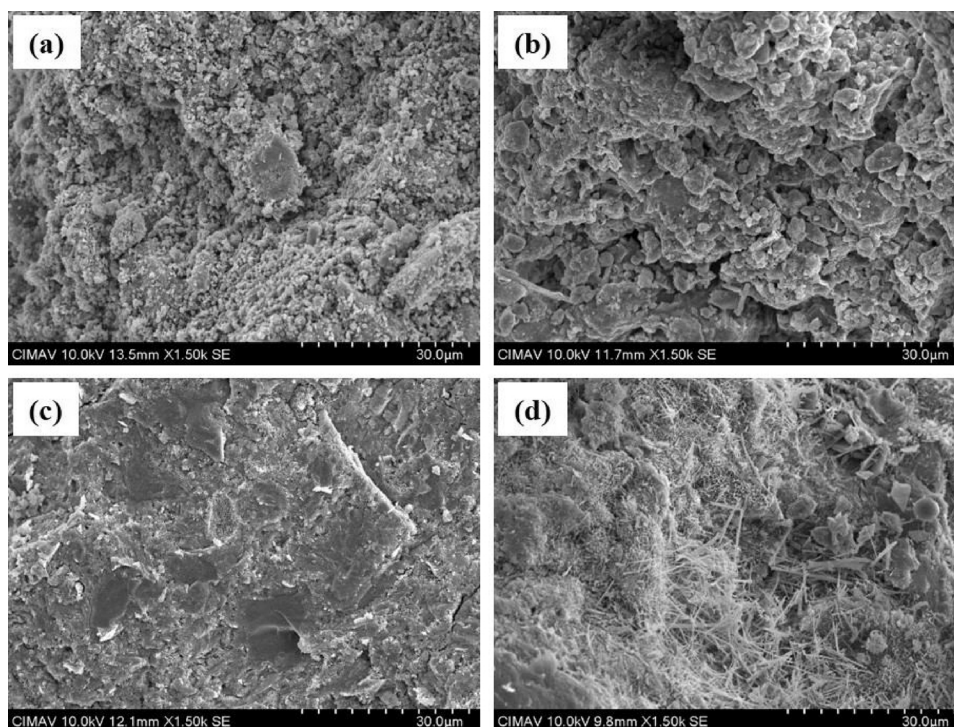

Fig. 9. SE-SEM micrographs of geopolymeric a) paste and b) mortar, and ordinary c) paste and d) mortar.

performance similar to that of the ordinary materials. In the case of the geopolymeric paste, its performance is better than the ordinary paste at early curing time (7 days). The similarity in the compression strength of geopolymeric materials with that of ordinary is favorable since it has been shown that the production of geopolymers generates a lower amount of greenhouse gases. Fig. 9 shows micrographs of the compression fracture morphology of finished products, both geopolymeric and ordinary pastes and mortars.

In addition to all results reported in this work, an economic analysis would be desirable. According to the literature, the production cost of geopolymers depends on the raw material used, source location, the energy source and transportation [14]. For example, fly ash sources have increased their cost and variability in recent years, making the search for alternative raw materials, as in our case where we use silica-rich sand of the region to synthesize the Na_2SiO_3. The financial costs of geopolymers could be 7% lower than OPC [14]. Also, Duxon et al. [28] say that, for the case of geopolymeric concrete derived from fly ash, the cost of the material is generally about 10–30% less than OPC. The OPC production cost also varies between US\$ 35.00 and US\$ 40.00 per ton of cement depending on the capacity [29]. Therefore, the production cost of 1 ton of geopolymer could vary between US\$ 24.50 and US\$ 37.20.

4. Conclusions

This study is devoted to compare the CO_2 emissions produced during the synthesis of a geopolymer and an ordinary Portland cement, through thermogravimetry. However, the analysis is focused on the decarbonation step, where almost all CO_2 emissions are generated. The energy to produce a geopolymer is less than that to produce an ordinary Portland cement. The main contributors to the environmental pollution are the CO_2 emissions from the decarbonation process; in addition, one need to consider the emissions due to processing temperature. The geopolymer is processed at about 600 °C lower temperature than the Portland cement. The decarbonation process for the geopolymer generates 45% less CO_2 than the clinker and another 9% is associated to the differences in temperature. Therefore, the geopolymer generates 54% less CO_2 than the clinker. Here we demonstrate that thermogravimetry is a reliable method to accurately measure CO_2 emissions. These results, together with those of the compression strength, allow to conclude that geopolymers can be suitable alternatives to substitute ordinary cements.

Acknowledgements

References

[1] Á.V. Ortuño, Introducción a la química industrial, (1998) Barcelona, España: Reverté.
[2] E.C. Eckel, Portland cement materials and industry in the United States, US Government Printing Office, 1913.
[3] J. Newman, B.S. Choo, Advanced Concrete Technology vol. 4, Butterworth-Heinemann, 2003.
[4] M. Hassaan, Effect of gypsum on the strength development of portland cement by Mössbauer spectrometry, Hyperfine Interact. 42 (1) (1988) 1199–1202.
[5] E. Gartner, Industrially interesting approaches to "low-CO2" cements, Cem. Concr. Res. 34 (9) (2004) 1489–1498.
[6] M. Abdullah, et al., Asas Geopolimer (Teori & Amali), Unit Penerbitan Universiti Malaysia Perlis, Perlis, 2013.
[7] D. Hardjito, Studies of Fly Ash-based Geopolymer Concrete, Curtin University of Technology, Sydney, 2005 PhD thesis.
[8] R. Anuradha, et al., Modified guidelines for geopolymer concrete mix design using Indian standard, Asian J. Civil Eng. (Build. Hous.) 13 (3) (2012) 353–364.
[9] A. Rahman, et al., Impact of alternative fuels on the cement manufacturing plant performance: an overview, Procedia Eng. 56 (2013) 393–400.
[10] L.K. Turner, F.G. Collins, Carbon dioxide equivalent (CO2-e) emissions: a comparison between geopolymer and OPC cement concrete, Constr. Build. Mater. 43 (2013) 125–130.
[11] E. Benhelal, et al., Global strategies and potentials to curb CO2 emissions in cement industry, J. Clean. Prod. 51 (2013) 142–161.
[12] R. Nowak, Geopolymer concrete opens to reduce CO2 emissions, New Sci. 197 (2640) (2008) 28–29.
[13] J. Provis, J. Van Deventer, Geopolymers: Structure, Processing, Properties and Industrial Applications, Woodhead Publishing Limited, 2009.
[14] B.C. McLellan, et al., Costs and carbon emissions for geopolymer pastes in comparison to ordinary portland cement, J. Clean. Prod. 19 (9) (2011) 1080–1090.
[15] A. Fernández-Jiménez, A. Palomo, D. Revuelta, Alkali activation of industrial by-products to develop new earth-friendly cements, Proceedings of the 11th International Conference on Non-Conventional Materials And Technologies (NOMAT 2009), (2009).
[16] J.L. Provis, J.S. van Deventer, Designing green construction materials through reaction engineering, 8th World Congress of Chemical Engineering. Montreal, Canada, CD-ROM Proceedings, (2009).
[17] J. Davidovits, The need to create a new technical language for the transfer of basic scientific information, Transfer and Exploitation of Scientific and Technical Information, EUR Vol. 7716 (1982), pp. 316–320.
[18] B. Singh, et al., Geopolymer concrete: a review of some recent developments, Constr. Build. Mater. 85 (2015) 78–90.
[19] M.M. Al Bakri, et al., Review on fly ash-based geopolymer concrete without Portland Cement, J. Eng. Technol. Res. 3 (1) (2011) 1–4.
[20] J. Davidovits, Geopolymer Chemistry and Applications, FR: Geopolymer Institute, Saint-Quentin, 2008 ISBN 978-2-9514820-1-2.
[21] M. Rowles, B. O'connor, Chemical optimisation of the compressive strength of aluminosilicate geopolymers synthesised by sodium silicate activation of meta-kaolinite, J. Mater. Chem. 13 (5) (2003) 1161–1165.
[22] L. Guiping, Material and manufacturing technology II: selected, Peer reviewed papers from the 2011, 2nd International Conference on Material and Manufacturing Technology (ICMMT 2011), July 8-11, 2011, Xiamen, China, 2012 Trans Tech Publications.
[23] A.S.T.M. C114-15, Standard Test Methods for Chemical Analysis of Hydraulic Cement, ASTM International, 2015.
[24] P.A. Gerakines, et al., The Infrared Band Strengths of H2O, CO and CO2 in Laboratory Simulations of Astrophysical Ice Mixtures, arXiv preprint astro-ph/9409076 (1994).
[25] O. Vázquez, B. Del Valle, El desarrollo de líneas base para el sector energético y conmparación con el sector de uso de suelos. Asociacion de Tecnicos y Profesionistas en Aplicacion Energetica (ATPAE), Available from: (2010) http://www.inecc.gob.mx/descargas/cclimatico/10%20Presentaci%F3n%20ATPAE-EnergySector.pdf.
[26] J.B. Nelson, Molten salt synthesis for manufacture of cement precursors. Patent US20150299040 A1. 2014.
[27] A. Hasanbeigi, L. Price, E. Lin, Emerging energy-efficiency and CO2 emission-reduction technologies for cement and concrete production: a technical review, Renew. Sustain. Energy Rev. 16 (8) (2012) 6220–6238.
[28] P. Duxson, et al., Geopolymer technology: the current state of the art, J. Mater. Sci. 42 (9) (2007) 2917–2933.
[29] Settlements, U.N.C.f.H, Small-scale Production of Portland Cement, United Nations Centre for Human Settlements (Habitat), 1993.